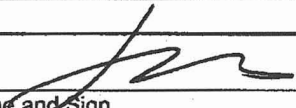
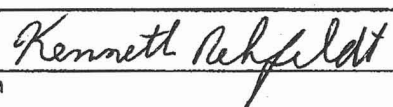

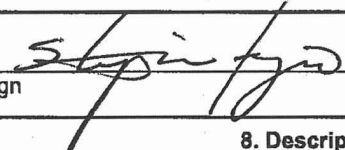




**Scientific Analysis/Calculation
Administrative Change Notice**

QA: QA
Page 1 of 1

Complete only applicable items.

1. Document Number: ANL-NBS-HS-000058		2. Revision: 00	3. ACN: 01
4. Title: Calibrated Unsaturated Zone Properties			
5. No. of Pages Attached: 21			
6. Approvals:			
Preparer: <u>H. H. Liu</u>  <u>7/2/07</u> Print Name and Sign Date			
Checker: <u>Kenneth Rehfeldt</u>  <u>7/2/2007</u> Print name and sign Date			
QCS/Lead Lab QA Reviewer: <u>Charles Beach</u>  <u>7/3/07</u> Print name and sign Date			
Responsible Manager: <u>Stephanie Kuzio</u>  <u>7/10/07</u> Print name and sign Date			
7. Affected Pages		8. Description of Change:	
4-1, 4-2, 4-8, 4-9, 6-1, 6-2, 6-3, 6-5, 6-9, 6-9a, 6-11, 6-15, 6-29, 6-30, D-1, D-2, D-3, D-4, G-1, G-3, G-4		Changes incorporate formal DOE comments and are either editorial or provide additional clarification.	

4. INPUTS

This section discusses input data and parameters used in this report.

4.1 DIRECT INPUTS

Source information on the direct inputs is summarized in Table 4-1 and is further documented below. Specific data files from each data set (Table 4-1) used in this study, are described in Section 6 and/or the related appendices. The appropriateness of the inputs is also described.

4.1.1 Output from Other Models and Analyses

Developed data include the spatially varying infiltration maps from the infiltration model and several numerical grids, which are documented in separate reports (BSC 2004 [DIRS 169855]; SNL 2007 [DIRS 174294]). These data sets are too large to reproduce here, but are listed by data tracking number (DTN) in Table 4-1. Uncalibrated properties and property-estimate uncertainties of the matrix and fractures, which are used as inputs to the calibration, are listed in Tables 4-2 and 4-3, respectively. Porosity, residual saturation, saturated saturation, and van Genuchten parameter m are not calibrated. All other properties and uncertainty data are used to constrain the calibration. The appropriateness of the numerical grids for simulating flow and transport in the unsaturated zone is presented in a scientific analysis report (BSC 2004 [DIRS 169855]).

4.1.2 Acquired Data

Acquired data include saturation; water potential; pneumatic pressure; fracture, matrix, and fault properties; infiltration maps; and numerical grids. In all cases, the data sets are too large to reproduce here, but are listed by DTN in Table 4-1. These data are developed prior to use in the inversions as documented in Sections 6.2 and 6.3.4. Data that are not used are also discussed.

4.1.2.1 Saturation Data

Saturation data measured on core from boreholes USW SD-6, USW SD-7, USW SD-9, USW SD-12, USW UZ-14, UE-25 UZ#16, USW WT-24, USW UZ-N11, USW UZ-N31, USW UZ-N32, USW UZ-N33, USW UZ-N37, USW UZ-N38, USW UZ-N53, USW UZ-N54, USW UZ-N55, USW UZ-N57, USW UZ-N58, USW UZ-N59, and USW UZ-N61 are used for the one-dimensional inversions. The locations of these boreholes are shown in Figure 4-1. These boreholes do not intersect mapped faults, and thus the saturation data from these boreholes are representative of the rock mass of Yucca Mountain. Saturation data measured on core from Borehole USW UZ-7a (location shown in Figure 4-1) are used for the two-dimensional inversions. This borehole intersects the Ghost Dance fault, and saturation data from this borehole are judged to be representative of the faulted rock at Yucca Mountain.

Saturation data measured on core from several boreholes and tunnels at Yucca Mountain are not included in any of the inversions. Saturation data measured on core from boreholes USW NRG-6 and USW NRG-7a are not used because handling of the core caused excessive drying (Rousseau et al. 1999 [DIRS 102097], p. 125). Saturation data measured on core from the

Exploratory Studies Facility (ESF), Enhanced Characterization of Repository Block Cross-Drift, alcoves, and niches are not used, because they represent only a single layer in the stratigraphic column and are generally consistent with ranges of matrix saturation data collected from the boreholes (used for calibrations) for the given geological units. Geophysical measurements of saturation are not used because of larger uncertainties associated with these data, compared with direct measurements of saturation by oven drying. A detailed discussion of the relevant geophysical measurements was presented by *Thermal Conductivity of the Potential Repository Horizon* (BSC 2004 [DIRS 169854], Appendix B) as compared with the corresponding core measurements. The iTOUGH2 input files from DTNs: LB0208UZDSCPMI.001 [DIRS 161285], LB0208UZDSCPUI.001 [DIRS 166711], LB0302AMRU0035.001 [DIRS 162378] and LB02092DSSCFPR.001 [DIRS 162422] contain the saturation data formatted for iTOUGH2 inversions. In this study, these input files are used as the direct inputs into inversion runs. These DTNs are output from *Calibrated Properties Model* (BSC 2004 [DIRS 169857]). SCI-PRO-005, Section 6.2.1 D, states ‘if using a previously validated mathematical model to complete the scientific A/C [analysis or calculation], obtain the appropriate model file/product output from the Technical Data Management System (TDMS).’ The justification of the appropriateness to use these data is provided in Section 4.1.3.

Table 4-1. Input Data Sources and Data Tracking Numbers

DTN	Data Description	Section Describing Data Use
LB0208HYDSTRAT.001 [DIRS 174491]	2002 UZ Model Grid Components: Supporting Files	Appendix C
GS000608312261.001 [DIRS 155891]	In situ Pneumatic Pressure Data for Borehole UE-25 NRG#5	6.2.3
GS950208312232.003 [DIRS 105572]; GS951108312232.008 [DIRS 106756]; GS031208312232.007 [DIRS 178751]	In situ Pneumatic Pressure Data for Borehole USW NRG-6 & USW NRG-7a	6.2.3
GS960908312261.004 [DIRS 106784]	In situ Pneumatic Pressure Data for Borehole USW SD-7	6.2.3
GS031208312232.008 [DIRS 178750]	In situ Pneumatic Pressure Data for Borehole USW SD-12, USW NRG-7a, and USW UZ-7a	6.2.3 6.3.3 6.3.4
SN0609T0502206.028 [DIRS 178753]	Present-Day Infiltration Maps	6.2.5 Appendix C Appendix D Appendix F
LB02081DKMGRID.001 [DIRS 160108]	One-dimensional and two-dimensional grids	6.2.1 6.3.4 Appendix B Appendix F
LB0205REVUZPRP.001 [DIRS 159525]	Uncalibrated Fracture Property Data	6.4 Appendix F
LB0207REVUZPRP.002 [DIRS 159672]	Uncalibrated Matrix Property Data	6.4
LB0207REVUZPRP.001 [DIRS 159526]	Uncalibrated Fault Property Data	6.3.4

4.1.2.4 Use of Established Fact Data and the Data Qualified for the Intended Use

Established fact data are used in Equations 6-8 through 6-10 (Section 6.2.2). These data include physical properties of air, the molecular weight and critical temperature and critical pressure of both air and water, and the mole fraction of water vapor in air. The data values and sources are specified in Section 6.2.2 of this report.

Data used for determining uncertainties in measurements of matrix saturation and water potential (Flint 1998 [DIRS 100033], pp. 11, and 17 to 19; Rousseau et al. 1999 [DIRS 102097], pp. 129 to 131 and 144), as discussed in Section 6.2.2, are qualified for the intended use in this report (Appendix G).

4.1.3 Use of Technical Product Outputs (TPOs) from the Calibrated Properties Model

Inputs taken from *Calibrated Properties Model* (BSC 2004 [DIRS 169857]) and their usage in this current report are given in Table 4-4. Per SCI-PRO-005, *Scientific Analyses and Calculations*, these inputs are considered suitable for their intended uses in this report because they are the best available data for their intended purposes. Table 4-4 provides descriptions and specific justifications for using the input data files obtained from *Calibrated Properties Model* (BSC 2004 [DIRS 169857]).

Table 4-4. Input Data from Calibrated Properties Model Report

No	DTN	Data Description	Data Use and Additional Justifications
1	LB0208UZDSCPMI.001 [DIRS 161285]	Calibrated one-dimensional parameter set for base-case infiltration scenario (<i>minfl7Ddri.par</i>), and compiled water saturation and potential data (<i>minfl7Ddri</i>).	The parameter set was used as initial guesses for inverse modeling, and the formatted water saturation and potential data were used for parameter calibration. Selecting an initial guess that is close to the final value of the calibrated parameter improves the chance of finding a good match with observed data (see Section 6.3.2 and Appendix D). These data are considered the best available guesses, because they were derived through rigorous inverse modeling exercise that met all the quality assurance requirements in place at the time.
2	LB0208UZDSCPU1.001 [DIRS 166711]	Calibrated one-dimensional parameter set for upper-bound infiltration scenario (<i>UinfA1i.par</i>), and compiled water saturation and potential data (<i>UinfA1i</i>).	
3	LB02091DSSCP3I.001 [DIRS 161292] LB0302AMRU0035.001 [DIRS 162378]	Formatted gas pressure data (<i>*.txt</i> , <i>MinfGasAi</i> , <i>NMi</i>), and formatted boundary condition (<i>timvsp.dat</i>).	These compiled and formatted input files were directly used for one-dimensional, mountain-scale calibration (see Sections 6.3.3 and Appendix E). These input files were considered appropriate for their intended use in this report because they were derived from qualified data sources.

Table 4-4. Input Data from Calibrated Properties Model Report (Continued)

No	DTN	Data Description	Data Use and Additional Justifications
4	LB0210AMRU0035.002 [DIRS 166712]	Uncertainties for rock properties.	These property uncertainties were directly used for determining calibrated property uncertainties (section 6.4.2). They were considered appropriate for their intended use in this report because they were derived from qualified data sources.
5	LB02092DSSCFPR.001 [DIRS 162422]	Compiled saturation data and water potential data (<i>MFAi</i>), formatted pneumatic pressure data (<i>*.prm</i> ; <i>LMGi</i>), and boundary condition (<i>timvspF.dat</i>).	These compiled and formatted input files were directly used for calibration of fault parameters (see Section 6.3.4 and Appendix F). These input files were considered appropriate for their intended use in this report because they were derived from qualified data sources.

TPO=technical product output.

The results reported in *Calibrated Properties Model* (BSC 2004 [DIRS 169857]) have also been used in peer-reviewed journal publications for discussing unsaturated flow and transport processes in Yucca Mountain (Wu et al. 2004 [DIRS 156399]; Liu et al. 2004 [DIRS 166106]). Publication of these results in peer-reviewed journals provides additional confidence that the information is adequate and suitable for its intended use. Use of TPOs from other reports is discussed in Section 4.1.1.

4.2 CRITERIA

Technical requirements to be satisfied by performance assessment are based on 10 CFR 63.114 [DIRS 173273] (“Requirements for Performance Assessment”) and 10 CFR 63.115 [DIRS 173273] (“Requirements for Multiple Barriers”). The acceptance criteria that will be used by the U.S. Nuclear Regulatory Commission to determine whether the technical requirements for this report have been met are identified in *Yucca Mountain Review Plan, Final Report* (YMRP) (NRC 2003 [DIRS 163274]). The pertinent requirements and criteria for this analysis report are summarized in Table 4-5.

Table 4-5. Project Requirements and Yucca Mountain Review Plan Acceptance Criteria Applicable to This Report

Requirement	YMRP Acceptance Criteria ^a
10 CFR 63.114 (a and b)	Criteria 1, 2, and 3 for <i>Flow Paths in the Unsaturated Zone</i>

^aFrom NRC 2003 [DIRS 163274], Section 2.2.1.3.6.3.

The acceptance criteria identified in Section 2.2.1.3.6.3 of the YMRP (NRC 2003 [DIRS 163274]) are included below. In cases where subsidiary criteria are listed in the Yucca Mountain Review Plan for a given criterion, only the subsidiary criteria addressed by this scientific analysis are listed below. How these components are addressed is summarized in Section 7 of this report.

Acceptance Criteria from Section 2.2.1.3.6.3, *Flow Paths in the Unsaturated Zone*

Acceptance Criterion 1, *System Description and Model Integration Are Adequate.*

6. DISCUSSION

6.1 BACKGROUND

6.1.1 Objectives

The UZ models are used to represent past, present, and future hydrological, thermal-hydrological and chemical conditions within the unsaturated zone of Yucca Mountain. The UZ models consist of hydrological (flow and transport) and thermal properties, and a numerical grid, which together form input for the TOUGH family of simulators. This report documents the development of some of the hydrologic properties for the UZ models. Assumptions used in this section and their bases are presented in Section 5. The intended use of the output data developed using approaches in this section is given in Section 1.

6.1.2 Conceptual Model and Alternative Models

Property calibration of the UZ models is a key step in the model development. Property calibration is necessary to refine the property estimates derived from laboratory and field data, so they are suitable for use in the UZ models and so UZ models accurately depict hydrological conditions in the mountain. The UZ models consider large-scale hydrological processes; where properties are scale dependent, upscaling will inherently be part of the calibration process. The calibration process also reduces property-estimate uncertainty and bias. Property estimates from laboratory and field data, like any other estimates, will have uncertainty associated with them because of data limitations (e.g., sampling and measurement biases, limited number of samples). The conceptual model and numerical schemes used to develop the numerical representation of the UZ models have been documented in *Conceptual Model and Numerical Approaches for Unsaturated Zone Flow and Transport* (BSC 2004 [DIRS 170035]). The aspects of the conceptual model and numerical schemes that are most relevant to this study are highlighted in this section. Alternative models and numerical approaches are also discussed in this section.

A variety of numerical approaches have been proposed to deal with flow and transport processes in fractured media at field scale (BSC 2004 [DIRS 170035], Section 6.3.1). When classified according to the manner in which fracture networks are treated in the model structure, the approaches fall into three groups: (1) continuum approaches (including effective continuum, dual continuum, and multiple interacting continua), (2) discrete fracture-network approaches, and (3) other approaches (e.g., a combination of the continuum approaches and the discrete fracture-network approaches). Based on overall flow and transport behavior in the unsaturated zone, the scale of the problem under consideration, and a balance between simulation accuracy and computational feasibility, the dual-permeability method (a continuum approach) is considered appropriate for describing flow and transport in the unsaturated zone (BSC 2004 [DIRS 170035], Section 6.3.2). Consequently, the dual-permeability method is used for all the simulation studies documented in this report. The alternative approaches (including discrete fracture-network approaches and other approaches) generally involve computational generation of synthetic fracture networks and subsequent simulations of flow and transport in each individual fracture. While these approaches are useful as tools for concept evaluation, they are not practically feasible for dealing with large-scale problems (BSC 2004 [DIRS 170035], Section 6.3).

Because the Paintbrush nonwelded hydrogeologic unit (PTn) attenuates episodic infiltration pulses, liquid water flow below the PTn is considered to be approximately in steady state under ambient conditions (BSC 2004 [DIRS 170035], Sections 6.1.2 and 6.1.6). The ambient conditions refer to conditions under which flow and transport processes in the unsaturated zone are not disturbed by heat loading from nuclear wastes that are proposed to be stored in the repository horizons. This study focuses on flow processes and data collected under ambient conditions. Steady-state liquid flow conditions are thus used in all the studies documented in this report. Note that the existence of episodic flow through the PTn (possibly through faults) is indicated by the finding of potential “bomb-pulse” signature of ^{36}Cl in the unsaturated zone (BSC 2006 [DIRS 179489]). However, this flow component carries only a small amount of water (BSC 2004 [DIRS 170035], Sections 6.1.6 and 6.1.7).

Heterogeneities exist at different scales within both the fracture and matrix continua in the unsaturated zone at Yucca Mountain. Treatment of subsurface heterogeneity and parameterization (use of a number of parameters to represent the heterogeneous distribution) is highly relevant to calibration of hydraulic properties. A geologic-based, deterministic approach is mainly used for characterizing subsurface heterogeneity in the unsaturated zone (BSC 2004 [DIRS 170035], Section 6.3.4). This is based on the following considerations: (1) overall behavior of large-scale flow and transport processes are mainly determined by relatively large-scale heterogeneities associated with the geologic structures of the mountain, (2) the heterogeneity model needs to be consistent with the available data, and (3) this approach is also supported by field observation (e.g., matrix-saturation distributions) (BSC 2004 [DIRS 170035], Section 6.3.4). Therefore, the heterogeneity of hydrological properties in this study is treated as a function of geologic layering, shown in Table 6-3, so that any one geologic layer has homogeneous properties (referred to as layer average properties), except where faulting or variable alteration (e.g., zeolitization) is present. In these cases, two sets of properties are used for layers with variable alteration, one for the portion of the layer that is altered beyond some threshold and one for the remaining portion. *Development of Numerical Grids for UZ Flow and Transport Modeling* (BSC 2004 [DIRS 169855], Section 6) documents this process. Heterogeneity in faults is treated as a function of major hydrogeologic units shown in Table 6-1, with the Calico Hills nonwelded hydrogeologic unit (CHn) and CFu combined (i.e., only four sets of hydrological properties are used for the faults).

The van Genuchten (1980 [DIRS 100610], pp. 892 to 893) relations, originally developed for porous media, have been used as constitutive relationships for liquid flow in the unsaturated zone (BSC 2004 [DIRS 170035], Section 6.3.5). This treatment results from the use of porous-medium equivalence for describing flow in fractures. Recently, Liu and Bodvarsson (2001 [DIRS 160110]) developed a new constitutive-relationship model for unsaturated flow in fracture networks, based mainly on numerical experiments. They found that results of the van Genuchten model are close to their simulation results when the water saturation value is small, which indicates that the van Genuchten model is approximately valid for low fracture saturations corresponding to ambient conditions. Therefore, the van Genuchten model is still used in this study. Calibrations are performed using data collected under ambient conditions.

In a number of laboratory scale experiments, Glass et al. (1996 [DIRS 139237]) demonstrated that gravity-driven fingering flow is a common flow mechanism in individual fractures. Fingering flow can occur at different scales. It has been well known in the subsurface hydrology community that flow and transport processes and the related parameters are scale-dependent

(e.g., Neuman 1994 [DIRS 105731]). Fingering flow at a fracture network scale, resulting from subsurface heterogeneity and nonlinearity involved in an unsaturated system, is a more important mechanism for liquid flow in the unsaturated zone than fingering flow in individual fractures. This is because the UZ flow model deals with flow and transport at large scales consisting of a great number of fractures. The active fracture model of the report by Liu et al. (1998 [DIRS 105729]) is used for considering the mechanism of fingering flow at a fracture network scale (BSC 2004 [DIRS 170035], Section 6.3.7). The active fracture concept is based on the reasoning that, as a result of fingering flow, only a portion of fractures in a connected, unsaturated fracture network contributes to liquid water flow. A detailed evaluation of the active fracture model based on both theoretical arguments and field observations is presented in *Conceptual Model and Numerical Approaches for Unsaturated Zone Flow and Transport* (BSC 2004 [DIRS 170035], Section 7).

Liquid flow occurs predominantly in the matrix in the non-welded PTn and the matrix in vitric portions of the CHn. The dominant matrix flow results from relatively high matrix permeabilities and low fracture densities in these units (BSC 2004 [DIRS 170035], Section 6.1.2). In the welded units (layers), liquid flow occurs predominantly in the fractures. This conceptual model is supported by UZ flow tests conducted in nonwelded tuffs at Busted Butte and in the ESF Alcove 4. The tests at Busted Butte conducted in the upper CHn(v) show that flow took place in the matrix; fracture flow was not observed, given the limits of the observational capability (even though fractures are present) (BSC 2004 [DIRS 170004], Section 6.13). Tests in ESF Alcove 4 conducted in the PTn unit also show that flow around a large, through-going fracture is matrix-dominant (BSC 2004 [DIRS 170004], Section 6.7).

It is well known that permeability is scale-dependent (Neuman 1994 [DIRS 105731]). Calibrated properties are necessary on two scales, mountain-scale and drift-scale, to consider this scale-dependent behavior. Calibration of the mountain-scale properties considers pneumatic pressure data that reflect the mountain-scale process of barometric pumping. Mountain-scale properties are intended for use in models of processes at the mountain scale. Calibration of the drift-scale properties does not consider the pneumatic pressure data. Drift-scale properties are intended for use in models of processes at the drift scale.

6.1.3 Simulator and Numerical Model

In this study, iTOUGH2 V5.0 [DIRS 160106] is used for calibration. This program uses the integral-finite-difference method for spatial discretization, and is a general-purpose inverse and forward numerical simulator for multidimensional, coupled fluid and heat flow of multiphase, multicomponent fluid mixtures in porous and fractured media. To the best of the authors' knowledge, iTOUGH2 represents the state of the art in the area of inverse modeling of multiphase flow processes in fractured media. This code has been comprehensively tested under different conditions (Finsterle 1998 [DIRS 103783]; 1999 [DIRS 104367]). The forward flow simulation in iTOUGH2 V5.0 [DIRS 160106] involves numerically solving the following governing equation (for an arbitrary flow domain V_n with the boundary Γ_n) (Pruess 1987 [DIRS 100684], Section 3)

$$\frac{d}{dt} \int_{V_n} M dV = \int_{\Gamma_n} F \cdot n d\Gamma + \int_{V_n} q dV \quad (\text{Eq. 6-1})$$

multiphase flow in highly heterogeneous systems (Forsyth et al. 1995 [DIRS 161743]). Simulation of unsaturated flow in the unsaturated zone is numerically challenging because of a combination of heterogeneity and nonlinearity. To perform numerical simulation for such a complex system, both numerical accuracy and computational feasibility need to be considered. It is a reasonably practical choice to use this scheme to avoid the potential numerical problems. Secondly, use of the approach is not expected to result in significant errors for simulating matrix imbibition processes in the unsaturated zone. In nonwelded units, the flow mainly occurs in the matrix, and the flow component from fractures to the matrix is expected to be small (Section 6.1.2). In the welded units, flow mainly occurs in fractures (because of small matrix permeability), again resulting in a relatively small flow component from fractures to the matrix. Finally, the approximation introduced by the weighting scheme is also compensated by the calibration procedure, which includes the effects of numerical grids and numerical schemes.

Table 6-1. GFM2000 Lithostratigraphy, Unsaturated Zone Model Layer, and Hydrogeologic Unit Correlation

Major Unit (Modified from Montazer and Wilson 1984 [DIRS 100161])	GFM2000 Lithostratigraphic Nomenclature	Unsaturated Zone Model Layer	Hydrogeologic Unit (Flint 1998 [DIRS 100033], Table 1)
Tiva Canyon welded hydrogeologic unit (TCw)	Tpcr	tcw11	CCR, CUC
	Tpcp	tcw12	CUL, CW
	TpcLD		
	Tpcpv3	tcw13	CMW
	Tpcpv2		
Paintbrush nonwelded hydrogeologic unit (PTn)	Tpcpv1	ptn21	CNW
	Tpbt4	ptn22	BT4
	Tpy (Yucca)	ptn23	TPY
		ptn24	BT3
	Tpbt3		
	Tpp (Pah)	ptn25	TPP
	Tpbt2	ptn26	BT2
	Tptrv3		
	Tptrv2		
Topopah Spring welded hydrogeologic unit (TSw)	Tptrv1	tsw31	TC
	Tptrn	tsw32	TR
	Tptrl, Tptf	tsw33	TUL
	Tptpul, RHHtop		
	Tptpmn	tsw34	TMN
	Tptpll	tsw35	TLL
	Tptpln	tsw36	TM2 (upper 2/3 of Tptpln)

the mole fraction of water vapor in air far from the core, x_{∞} , is 0.0126 (Weast 1987 [DIRS 114295], p. D-190). The core surface area is approximately 297 cm² that is qualified for the intended use for this study in Appendix G. Using these values, an evaporation rate of 2.69×10^{-4} g-mole/s is calculated based on Equations 6-8 to 6-10.

At this evaporation rate, the saturation of a fully saturated core of matrix porosity 22.3% (a typical value for tuff matrix (Table 4-3)) will be reduced by 2.2% after 5 minutes, which is the handling time given by Flint (1998 [DIRS 100033], p. 11). A fully dry core will have no reduction in saturation. Using these two points, the linear dependence of saturation change on saturation yields the relation

$$\Delta S = 0.022S \quad (\text{Eq. 6-11})$$

where S is the uncorrected saturation value and ΔS is saturation change resulting from handling, or HE . Although the actual relation between ΔS and S may be much more complex than Equation 6-11, this equation is in practice adequate for estimating HE here. Average porosity for the entire mountain is calculated as a layer-thickness weighted average of individual layer porosities. Also, water lost to drilling air is not considered here, because an approach to accurately estimate water loss is not available. However, the estimation of HEs does not consider the effect of matrix water potential, resulting in overestimated handling errors. This may partially compensate for the effects of water lost to drilling air.

Rousseau et al. (1999 [DIRS 102097], p. 144) give ± 0.2 MPa as the 95% confidence interval (two standard deviations) for the in situ water-potential measurements. One standard deviation, 0.1 MPa, is used as an estimate for the uncertainty for the water potential. Also, the equilibrium (steady-state) water potential values used for calibration in this analysis report are consistent with more recent water potential data collected from April 1998 to December 2001 as shown in Appendix A.

6.2.3 Pneumatic Pressure Data

Thirty days of data from each borehole are used for the inversions. Several criteria are used to select data for the inversions: The data must include diurnal pressure changes and longer-period, weather-associated pressure changes; and must have been obtained prior to any influence from construction of the ESF. In this case, use of thirty days of data is sufficient for inversions of fracture permeabilities. Table 6-2 shows the starting and ending dates for the data that were used in the inversion. Data from the instrument station or port nearest the bottom of the Tiva Canyon welded hydrogeologic unit (TCw) are included because they show the lack of attenuation and lag in the barometric signal through the TCw. Data from stations between the lowermost in the TCw and the surface are not included, because they would not add information to the inversion and would weight the TCw data more than other data. Data from all instrument stations or ports in the PTn are included because there is substantial attenuation and lag in the barometric pumping signal through the PTn. Individual layers in the PTn are expected to have widely variable permeability, so it is important to include data that show the amount of barometric-signal attenuation and lag in different layers of the PTn. Data from the uppermost and lowermost instrument stations or ports in the TSw are included, because they show the lack of significant

attenuation and lag in the barometric pumping signal characteristics through the TSw. Data from the stations in between the uppermost and lowermost stations in the TSw unit

6.2.4 Prior Information

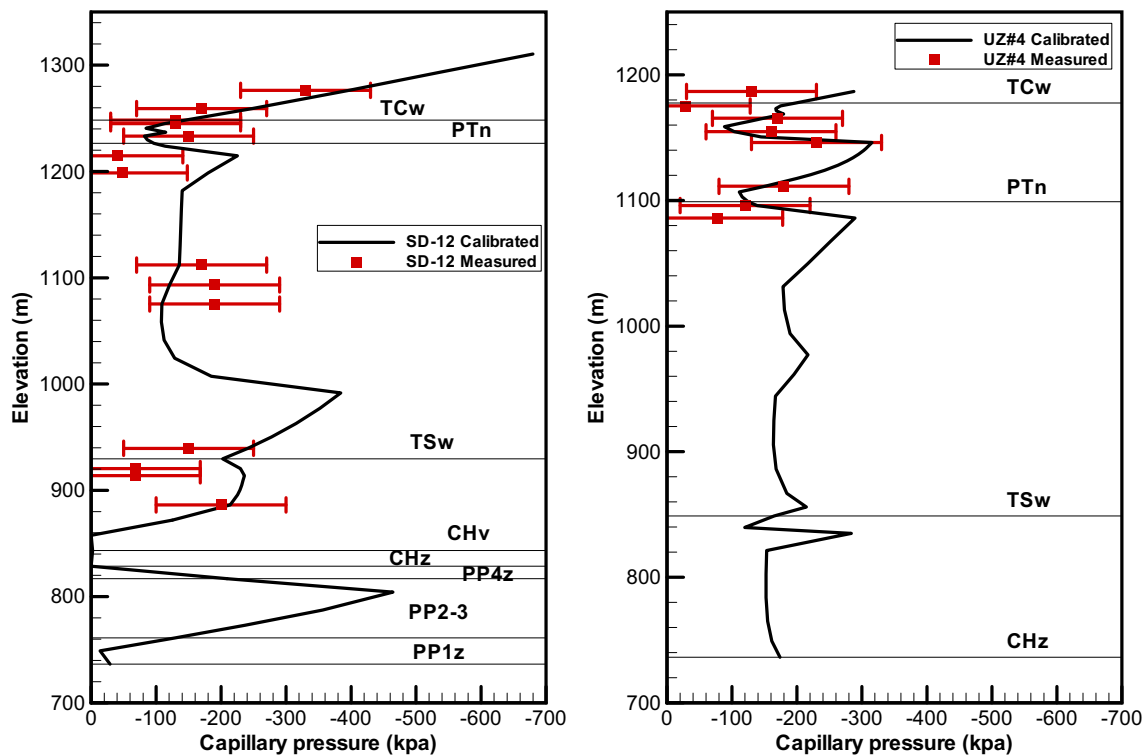
Uncalibrated rock-property data (Tables 4-3 and 4-4) are used as prior information. (Prior information refers to property data collected from both field and laboratory measurements.) In the inverting calculations reported in this report, the prior information is also used as direct input and data to be calibrated against. These data are just as important to the parameter calibration as data on the state of the system (e.g., saturation). The combination of the two types of information allows the calibration to match the data as close as possible, while simultaneously estimating rock parameters that are reasonable according to the prior information. Standard errors of parameters for weighting the prior information are taken from Tables 4-2 and 4-3. Matrix permeability data are weighted by the inverse of the standard error (Equation 6-7), giving more weight to the more certain measurements (Finsterle 1999 [DIRS 104367], Sections 1.5 and 2.5.3). Because permeability is lognormally distributed, σ and thus SE are estimated for the log-transformed permeabilities (i.e., $\log(k)$). The number of samples used for calculation of the standard error does not include nondetect samples (i.e., N in Equation 6-7 is the total number of samples minus the number of nondetect samples, as shown in Table 4-3). As discussed below, drift-scale fracture permeabilities are directly assigned from the prior information, and therefore standard error data are not needed for calibration of drift-scale fracture permeabilities. Mountain-scale fracture permeabilities, however, are calibrated using the pneumatic data, because the pneumatic data correspond to a mountain-scale process. In inversions of pneumatic pressure data, prior information does not significantly contribute to the objective function (Section 6.3.1) because the number of data points is considerably larger than the number of calibrated fracture permeabilities. Therefore, the choice of standard error used to weigh the prior information is inconsequential to the inversion. For simplicity, a standard error of two orders of magnitude is assigned to fracture permeabilities in TCw and PTn for calibrating mountain-scale nonfault property sets, and a standard error of one order of magnitude for calibrating fault property sets. For layers tsw31 through tsw37, fracture permeabilities are calibrated by a technique that does not require weighting, so no standard errors are used (see Section 6.3.3). Standard error is given for $\log(\alpha)$ because α is lognormally distributed. For fracture properties, the uncalibrated value of α_F is estimated based on fracture permeability and fracture frequency data (BSC 2004 [DIRS 170038], Section 6). Since a directly measured α_F value is not available, a relatively large value of 2 (or two orders of magnitude, compared with values for matrix $\log(\alpha)$) is assigned as standard error for $\log(\alpha_F)$ in inversions. These prior information data were incorporated and formatted in *minfl7Ddri* from DTN: LB0208UZDSCPMI.001 [DIRS 161285], *UinfAli* from DTN: LB0208UZDSCPUI.001 [DIRS 166711], *MinfGasAi* from DTN: LB02091DSSCP3I.001 [DIRS 161292], and *NMi* from DTN: LB0302AMRU0035.001 [DIRS 162378]. These files are used as direct inputs to inversion runs (Appendices D and E).

6.2.5 Boundary and Initial Conditions

Infiltration rates (DTN: SN0609T0502206.028 [DIRS 178753]) are used as top boundary conditions during calibration activities. To consider the uncertainty in infiltration rates, four infiltration maps (corresponding to the 10th, 30th, 50th, and 90th percentiles of probability distribution of the average infiltration rate) are used in this study. For each infiltration map (DTN: SN0609T0502206.028 [DIRS 178753]), the infiltration rate at each calibration borehole, shown in Table 6-3, is determined as an averaged infiltration-rate value over a circular area with a 200-m radius with the center at the borehole location (Appendix C). A relatively large value

Choice of Parameters for Calibration—Rock parameters to be estimated are matrix permeability, k , matrix van Genuchten parameter α (van Genuchten 1980 [DIRS 100610], pp. 892 to 893), fracture van Genuchten parameters α and an active-fracture-model parameter, γ (Liu et al. 1998 [DIRS 105729]) (values for $\log(k)$ and $\log(\alpha)$ are adjusted in inversions). Other parameters are not changed in the calibration. These parameters are calibrated for model layers shown in Table 6-1 (except the zeolitic portion of CHn), though in some cases a common parameter value is estimated for groups of layers. (Details regarding which layers are grouped for parameter estimation are discussed below.) Inverse modeling involves iterations through many forward simulations and is therefore computationally intensive. For computational efficiency, one-dimensional simulations are used because the time required for each forward simulation is relatively short (on the order of one minute) compared to two- and three-dimensional simulations. Thus, many simulations, thousands in this case, can be accomplished in a reasonably short period. The effect of using one-dimensional simulations is that all flow is forced to be vertical; no lateral flow is considered in these calibrations. From the surface to the repository, lateral flow is not expected to be significant because perched water has not been found here. Below the repository, in the Calico Hills nonwelded hydrogeologic unit (CHn: see Table 6-1) and the Crater Flat undifferentiated unit (CFu), areas of perched water exist where lateral flow may be significant. Properties needed to produce perched water and varying degrees of lateral flow within the CHn and CFu units are further refined during three-dimensional calibrations performed in *UZ Flow Models and Submodels* (SNL 2007 [DIRS 175177], Section 6). Properties for the zeolitic portion of CHn, the unit where perched water is observed, are not calibrated here. Fracture permeability and van Genuchten m are not calibrated here because they are relatively insensitive to simulated matrix-saturation and water-potential distributions (BSC 2004 [DIRS 169857], Section 6.3.3; Bandurraga and Bodvarsson 1999 [DIRS 103949], Section 5). Also, in the vitric part of the CHn, the fracture van Genuchten parameters α and an active-fracture-model parameter, γ , are not calibrated, because under the ambient conditions, water flow occurs mainly in the matrix (Section 6.1), and therefore these two parameters are not sensitive to simulated matrix saturation and water potential values. Furthermore, the field data in the vitric part of CHn are very limited. (For example, there are only 23 [out of total 298] matrix saturation data points in the vitric part of the CHn.) For a model layer where parameter γ is not calibrated, a parameter value of 0.25 is assigned to the layer, because the reasonable range of the parameter is between 0.2 and 0.4 for the unsaturated zone (BSC 2004 [DIRS 170035] Section 7) and 0.25 is close to the middle of the range. A detailed discussion on sensitivities of rock properties to the relevant simulation results is provided by Bandurraga and Bodvarsson (1999 [DIRS 103949], Section 5). Based on available data and previous calibrations (Bandurraga and Bodvarsson 1999 [DIRS 103949], Section 5), the set of parameters chosen for calibration has been shown to be adequate in representing ambient conditions in the unsaturated zone at Yucca Mountain.

Residual and saturated saturation are parameters that do not influence the calibration to ambient data as strongly as the van Genuchten parameter α . This is because ambient saturation and water-potential data are generally not at the extremes of the relationships where these bounding values play a stronger role. Like matrix porosity, matrix residual saturation is another property that is simple to measure with low error, so it makes more sense to calibrate the parameters that are not well constrained.



Output DTN: LB0612UZDSCP90.001 (*Sandia2R217C*, *Sandia2R217C.out* and *Sandia2R217Ci.out*).

Figure 6-8. Water-Potential Matches at Selected Boreholes for One-Dimensional, Drift-Scale, Calibrated Parameter Set for the 90th Percentile Infiltration Scenario

6.3.3 Calibration of Mountain-Scale Parameters

Scale Dependence of Fracture Permeability—It is well documented in the literature that large-scale effective permeabilities are generally larger than smaller-scale permeabilities (Neuman 1994 [DIRS 105731]). An intuitive explanation for this scale-dependent behavior is that a large observation scale, in an average sense, corresponds to a larger opportunity to encounter more permeable zones or paths when observations are made, which considerably increases the values of the observed permeability. Because of the scale difference, drift-scale fracture permeabilities, determined from air-injection tests, cannot be applied to mountain-scale simulations. Therefore, development of mountain-scale properties is needed. In addition to matching matrix-saturation and water-potential data, the determination of mountain-scale parameters also involves matching pneumatic pressure data measured in surface boreholes. In the drift-scale parameter sets, fracture permeabilities correspond to those determined from air-injection tests. The pneumatic pressure data result from mountain-scale gas-flow processes, whereas air-injection tests correspond to scales on an order of several meters or less.

Unlike the connected fracture networks and soils, studies on the scale-dependent behavior of matrix properties in unsaturated fractured rocks are limited. However, it is reasonable to believe that the scale-dependent behavior of the matrix is different from fracture networks. For example, relatively large fractures can act as capillary barriers for flow between matrix blocks separated

by these fractures, even when the matrix is essentially saturated (water potential is close to the air entry value). This might limit the matrix scale-dependent behavior to a relatively small scale associated with the spacing between relatively large fractures. Although it is expected that estimated large-scale matrix permeabilities should be larger than those measured on a core scale, no evidence exists to indicate that matrix properties should be very different on both the site and drift scales, which are much larger than the scale characterized by the fracture spacing. This point is also supported by the inversion results for the drift-scale properties. For example, the estimated matrix permeabilities are generally much closer to prior information than estimated site-scale fracture permeabilities.

Based on the above discussions, only fracture permeabilities for the mountain-scale property sets are recalibrated, whereas other properties remain the same as those in the corresponding drift-scale properties.

Calibration Procedure Using Pneumatic Pressure Data—The EOS3 module of iTOUGH2 V5.0 [DIRS 160106] is used for transient pneumatic simulations. Both the gas phase and the liquid phase are considered in the flow calculations. The pneumatic inversion is carried out in two steps. First, the fracture permeabilities for layers tcw11 through ptn26 are calibrated. Then, the permeabilities for layers tsw31 through tsw37 are calibrated as a group by multiplying the prior information for all seven layers by the same factor that is discussed later. The input and output data files for the calibration are documented in Appendix E in detail.

The calibrated fracture permeabilities resulting from inversion of pneumatic data are expected to be higher than the prior information, owing to the scale dependency of fracture permeabilities as described above. Therefore, the initial guesses for the fracture permeabilities are $\log(k) = -10.5$ for tcw11, tcw12, and tcw13, and $\log(k) = -11.5$ for ptn21 through ptn26. These estimates are higher than the corresponding prior information (Table 4-4). The permeabilities of layers tsw31 through 37 are set to the values previously calibrated using the pneumatic data (Appendix E).

The lack of significant attenuation in the TSw unit is considered an important feature shown by the gas pressure data. The calibrated fracture permeabilities for the model layers in the TSw unit need to be consistent with this feature. Therefore, fracture permeabilities in the TSw should be determined in such a way that the simulated and observed gas pressure signals at the upper and lower sensor locations in the TSw have similar degrees of attenuation for Borehole USW SD-12. Borehole USW SD-12 is chosen for this analysis because the distance between the two TSw sensors within this borehole is the largest among all the relevant boreholes. The degree of attenuation of the barometric signal through the TSw in USW SD-12, or the relative difference between the signals at the two sensor locations, was determined by using standard functions of Excel® software (see description of *R113_d_factor_gaslibration.xls* in Section E3.5) to evaluate:

$$F = \frac{1}{N} \left\{ \sum_{i=1}^N [(P_u(t_i) - P_u(t_1)) - (P_b(t_i) - P_b(t_1))]^2 \right\}^{1/2} \quad (\text{Eq. 6-12})$$

where N is the total number of calibration time points, P is the gas pressure, and subscripts u and b refer to the sensors in the upper and lower (bottom) portions of the TSw within Borehole USW

This appendix describes input and output files for calibrations of drift-scale properties (Section 6). An iTOUGH2 run generally needs two input files—one containing rock property, numerical grid, source term, and initial conditions; another containing variables to be calibrated and data information used for calibration. For convenience, the first file is called a TOUGH2 input file, and the other, an iTOUGH2 input file.

D.1 CALIBRATION FOR THE 10TH PERCENTILE INFILTRATION MAP

All the input and output files discussed in this section have been submitted to TDMS under DTN: LB0610UZDSCP10.001.

The infiltration maps are from DTN: SN0609T0502206.028 [DIRS 178753]. As discussed in Appendix C, GENER block is generated based on the coordinates of the 20 calibration boreholes and the 10th percentile infiltration map.

The ROCKS block in the TOUGH2 input file is constructed from the calibrated rock property set for the USGS base-case infiltration rate, corresponding to DTN: LB0208UZDSCP10.001 [DIRS 161285] and *minfI7Ddri.par*. This is because the mean 10th percentile infiltration rate is close to the mean value for the USGS base-case infiltration map (Appendix C). Note that this previously calibrated property set is used as the initial guesses in the inversion herein. The numerical grid for one-dimensional calibration is discussed in Appendix B.

The iTOUGH2 input file in DTN: LB0208UZDSCP10.001 ([DIRS 161285], *minfI7Ddri*) is slightly modified for this calibration. The modifications include:

1. Combining the previous 16 calibration boreholes (NRG-6, SD-6, SD-7, SD-9, SD-12, UZ#4, UZ-14, UZ#16, UZN11, UZN31, UZN33, UZN37, UZN53, UZN57, UZN61, and WT-24) with the previous validation boreholes UZN32, UZN38, UZN54, UZN55, UZN58, UZN59, NRG-7a, and considering all of them to be calibration boreholes.
2. Using previous calibration results as the initial guess for property calibration (DTN: LB0208UZDSCP10.001 [DIRS 161285], *minfI7Ddri.par*)
3. Performing minor modifications to the “first GUESS” block to avoid convergence problem.

The input and output files for the five sequential calibration runs are listed in Table D-1. The number of sequential runs is determined by the criterion that the objective function is minimized and the calibrated properties are within reasonable ranges. For each run, the calibrated results in the *.par file of its previous run is used for the “first GUESS” block in the iTOUGH2 file. During the calibration, the objective function value is changed from 0.8493×10^4 (*Sandia2R218i.out*) to 0.6620×10^4 (*Sandia2R218Di.out*).

Table D-1. Input and Output Files for 10th Percentile Infiltration Map

Run1	Run2	Run3	Run4	Run5
<i>Sandia2R218</i>	<i>Sandia2R218A</i>	<i>Sandia2R218B</i>	<i>Sandia2R218C</i>	<i>Sandia2R218D</i>
<i>Sandiar2R218.out</i>	<i>Sandiar2R218A.out</i>	<i>Sandiar2R218B.out</i>	<i>Sandiar2R218C.out</i>	<i>Sandiar2R218D.out</i>
<i>Sandiar2R218.sav</i>	<i>Sandiar2R218A.sav</i>	<i>Sandiar2R218B.sav</i>	<i>Sandiar2R218C.sav</i>	<i>Sandiar2R218D.sav</i>
<i>Sandia2R218i</i>	<i>Sandia2R218Ai</i>	<i>Sandia2R218Bi</i>	<i>Sandia2R218Ci</i>	<i>Sandia2R218Di</i>
<i>Sandia2R218i.par</i>	<i>Sandia2R218Ai.par</i>	<i>Sandia2R218Bi.par</i>	<i>Sandia2R218Ci.par</i>	<i>Sandia2R218Di.par</i>
<i>Sandia2R218i.tec</i>	<i>Sandia2R218Ai.tec</i>	<i>Sandia2R218Bi.tec</i>	<i>Sandia2R218Ci.tec</i>	<i>Sandia2R218Di.tec</i>
<i>Sandia2R218i.out</i>	<i>Sandia2R218Ai.out</i>	<i>Sandia2R218Bi.out</i>	<i>Sandia2R218Ci.out</i>	<i>Sandia2R218Di.out</i>

D.2 CALIBRATION FOR THE 30TH PERCENTILE INFILTRATION MAP

All the input and output files discussed in this section have been submitted to TDMS under DTN: LB0610UZDSCP30.001.

The infiltration maps are from the DTN: SN0609T0502206.028 [DIRS 178753]. As discussed in Appendix C, GENER block is generated based on the coordinates of the 20 calibration boreholes and the 30th percentile infiltration map.

The ROCKS block in the TOUGH2 input file is constructed from the calibrated rock property set for the USGS upper-bound infiltration rate, corresponding to DTN: LB0208UZDSCPUI.001 [DIRS 166711] and *UinfAli.par*. This is because the mean 30th percentile infiltration rate is close to the mean value for the USGS upper infiltration map (Appendix C). Note that this previously calibrated property set is used as the initial guesses in the inversion herein. The numerical grid for one-dimensional calibration is discussed in Appendix B.

The iTOUGH2 input file in DTN: LB0208UZDSCPUI.001 [DIRS 166711], *UinfAli* is slightly modified for this calibration. The modifications include:

1. Combining the previous 16 calibration boreholes (NRG-6, SD-6, SD-7, SD-9, SD-12, UZ#4, UZ-14, UZ#16, UZN11, UZN31, UZN33, UZN37, UZN53, UZN57, UZN61, and WT-24) with the previous validation boreholes UZN32, UZN38, UZN54, UZN55, UZN58, UZN59, NRG-7a, and considering all of them to be calibration boreholes.
2. Using previous calibration results as the initial guess for property calibration (DTN: LB0208UZDSCPUI.001 [DIRS 166711], *UinfAli.par*)
3. Performing minor modification in the “first GUESS” block to avoid convergence problem.

The input and output files for the two sequential calibration runs are listed in Table D-1. The number of sequential runs is determined by the criterion that the objective function is minimized and the calibrated properties are within reasonable ranges. For each run, the calibrated results in the *.par file of its previous run is used for the “first GUESS” block in an iTOUGH2 file. During the calibration, the objective function value is changed from 0.8457×10^4 (*Sandia2R113i.out*) to 0.7551×10^4 (*Sandia2R113Ai.out*).

Table D-2. Input and Output Files for 30th Percentile Infiltration Map

Run1	Run2
<i>Sandia2R113</i>	<i>Sandia2R113A</i>
<i>Sandiar2R113.out</i>	<i>Sandiar2R113A.out</i>
<i>Sandiar2R113.sav</i>	<i>Sandiar2R113A.sav</i>
<i>Sandia2R113i</i>	<i>Sandia2R113Ai</i>
<i>Sandia2R113i.par</i>	<i>Sandia2R113Ai.par</i>
<i>Sandia2R113i.tec</i>	<i>Sandia2R113Ai.tec</i>
<i>Sandia2R113i.out</i>	<i>Sandia2R113Ai.out</i>

D.3 CALIBRATION FOR THE 50TH PERCENTILE INFILTRATION MAP

All the input and output files discussed in this section have been submitted to TDMS under DTN: LB0611UZDSCP50.001.

The infiltration maps are from the DTN: SN0609T0502206.028 [DIRS 178753]. As discussed in Appendix C, GENER block is generated based on the coordinates of the 20 calibration boreholes and the 50th percentile infiltration map.

The ROCKS block in the TOUGH2 input file is constructed from the calibrated rock property set for the USGS upper-bound infiltration rate, corresponding to DTN: LB0208UZDSCPUI.001 [DIRS 166711] and *UinfAi.par*. This is because the mean 50th percentile infiltration rate is close to the mean value for the USGS upper infiltration map (Appendix C). Note that this previously calibrated property set is used as the initial guesses in the inversion herein. The numerical grid for one-dimensional calibration is discussed in Appendix B.

The iTOUGH2 input file in DTN: LB0208UZDSCPUI.001 ([DIRS 166711], *UinfAi*) is slightly modified for this calibration. The modifications include:

1. Combining the previous 16 calibration boreholes (NRG-6, SD-6, SD-7, SD-9, SD-12, UZ#4, UZ-14, UZ#16, UZN11, UZN31, UZN33, UZN37, UZN53, UZN57, UZN61, and WT-24) with the previous validation boreholes UZN32, UZN38, UZN54, UZN55, UZN58, UZN59, NRG-7a and considering all of them to be calibration boreholes.
2. Using previous calibration results as the initial guess for property calibration (DTN: LB0208UZDSCPUI.001 [DIRS 166711], *UinfAi.par*)
3. Performing minor modification in the “first GUESS” block to avoid convergence problem.

The input and output files for the three sequential calibration runs are listed in Table D-1. The number of sequential runs is determined by the criterion that the objective function is minimized and the calibrated properties are within reasonable ranges. For each run, the calibrated results in the *.par file of its previous run is used for the “first GUESS” block in an iTOUGH2 file. During the calibration, the objective function value is changed from 0.9805×10^4 (*Sandia2R118i.out*) to 0.8460×10^4 (*Sandia2R118Bi.out*).

Table D-3. Input and Output Files for 50th Percentile Infiltration Map

Run1	Run2	Run3
<i>Sandia2R118</i>	<i>Sandia2R118A</i>	<i>Sandia2R118B</i>
<i>Sandiar2R118.out</i>	<i>Sandiar2R118A.out</i>	<i>Sandiar2R118B.out</i>
<i>Sandiar2R118.sav</i>	<i>Sandiar2R118A.sav</i>	<i>Sandiar2R118B.sav</i>
<i>Sandia2R118i</i>	<i>Sandia2R118Ai</i>	<i>Sandia2R118Bi</i>
<i>Sandia2R118i.par</i>	<i>Sandia2R118Ai.par</i>	<i>Sandia2R118Bi.par</i>
<i>Sandia2R118i.tec</i>	<i>Sandia2R118Ai.tec</i>	<i>Sandia2R118Bi.tec</i>
<i>Sandia2R118i.out</i>	<i>Sandia2R118Ai.out</i>	<i>Sandia2R118Bi.out</i>

D.4 CALIBRATION FOR THE 90TH PERCENTILE INFILTRATION MAP

All the input and output files discussed in this section have been submitted to TDMS under DTN: LB0612UZDSCP90.001.

The infiltration maps are from the DTN: SN0609T0502206.028 [DIRS 178753]. As discussed in Appendix C, GENER block is generated based on the coordinates of the 20 calibration boreholes and the 90th percentile infiltration map.

The ROCKS block in the TOUGH2 input file is constructed from the calibrated rock property set for the USGS upper-bound infiltration rate, corresponding to DTN: LB0208UZDSCPUI.001 [DIRS 166711] and *UinfAi.par*. This is because the mean 90th percentile infiltration rate is close to the mean value for the USGS upper infiltration map (Appendix C). Note that this previously calibrated property set is used as the initial guesses in the inversion herein. The numerical grid for one-dimensional calibration is discussed in Appendix B.

The iTOUGH2 input file in DTN: LB0208UZDSCPUI.001 ([DIRS 166711], *UinfAi*) is slightly modified for this calibration. The modifications include:

1. Combining the previous 16 calibration boreholes (NRG-6, SD-6, SD-7, SD-9, SD-12, UZ#4, UZ-14, UZ#16, UZN11, UZN31, UZN33, UZN37, UZN53, UZN57, UZN61, and WT-24) with the previous validation boreholes UZN32, UZN38, UZN54, UZN55, UZN58, UZN59, NRG-7a, and considering all of them to be calibration boreholes.
2. Using previous calibration results as the initial guess for property calibration (DTN: LB0208UZDSCPUI.001 [DIRS 166711], *UinfAi.par*)
3. Performing some minor modifications in the “first GUESS” block to avoid convergence problem.

The input and output files for the three sequential calibration runs are listed in Table D-4. The number of sequential runs is determined by the criterion that the objective function is minimized and the calibrated properties are within reasonable ranges. For each run, the calibrated results in the *.par file of its previous run is used for the “first GUESS” block in an iTOUGH2 file. During the calibration, the objective function value is changed from 0.1232×10^5 (*Sandia2R217i.out*) to 0.8538×10^4 (*Sandia2R217Ci.out*).

G.1 PURPOSE

This appendix documents qualification of data used to calculate weights given to observations in inverse modeling in Section 6.2.2. The values to be qualified are (a) the relative humidity, wind speed, and air temperature (of the environment in which samples were handled in the field) of 25%, 3 km/hr, and 30°C, respectively; (b) the core surface area available for evaporative loss of moisture of 297 cm²; (c) a 95% confidence for in situ measurement of water potential of ±0.2 MPa; (d) a sample handling time in the field of 5 min; and (e) error in measurement of saturation of 0.5%.

G.2 QUALIFICATION PLAN AND CRITERIA

Data Qualification Plan, Qualification of Parameter Values Used to Estimate Measurement Errors for Matrix Water Saturation and Water Potential (SNL 2006 [DIRS 178762]), hereafter called the data qualification plan, states that the qualification process will be according to Method 2 “Corroborating Data” in SCI-PRO-001, *Qualification of Unqualified Data*, Attachment 3, because data are available to conduct data comparisons that can be shown to substantiate or confirm parameter values. In addition, the data qualification plan (SNL 2006 [DIRS 178762]) states that Qualification Process Attribute 6 “the extent to which conditions under which the data were generated may partially meet the QA program that supports the YMP License Application process or post closure science” is used.

G.3 DATA QUALIFICATION DETAIL

G.3.1 Relative Humidity, Temperature, and Wind Speed

Relative humidity, temperature and wind speed data are used in Section 6.2.2 to estimate moisture loss during handling of rock core-samples when they are collected from the field. Corroborating data that support the relative humidity, temperature, and wind speed values used in the calculations in Section 6.2.2 were recorded at six sites at Yucca Mountain (DTN: SN0608WEATHER1.005 [DIRS 177912]). This qualified DTN was used in lieu of the DTNs provided in the data qualification plan (SNL 2006 [DIRS 178762]), which are not qualified. Sites 1, 2, and 9 were used for corroborating the unqualified data.

From the hourly-averaged relative humidity, temperature, and wind-speed data, those collected during daytime (8:00 AM to 6:00 PM, the most likely times of field work of collecting rock core-samples) were selected. From these, the minimum and maximum values of relative humidity, wind-speed data, and temperature for each site and year were identified and are summarized in Tables G-1, G-2, and G-3, respectively. The relative humidity, wind speed, and air temperature values used in the calculations of moisture loss in Section 6.2.2 (25%, 30°C, and 3 km/hr, respectively) are all within the range of observations obtained from the qualified data source and, therefore, meet the criteria for qualification of unqualified data provided in the data qualification plan (SNL 2006 [DIRS 178762]).

Calculation Procedures

The data reduction procedures employed were identical for all the three quantities (relative humidity, temperature, and wind speed). The following steps are used to calculate temperature:

Table G-3. Maximum and Minimum of Hourly-Averaged Day-Time Temperature (°C)

Site		1993	1994	1995	1996	1997	1998	1999	2000	2001	2002	2003	2004
1	Max	39.4	39.8	40.2	39.8	39.5	41.5	40.5	41.0	41.1	42.3	41.6	39.6
	Min	-6.2	-3.7	-2.6	-5.5	-7.7	-7.6	-2.3	-2.5	-2.7	-4.8	-3.2	-5.4
2	Max	36.4	38.8	38.3	38.2	37.8	39.8	38.3	38.8	38.9	39.9	39.7	37.5
	Min	-6.3	-4.4	-2.3	-5.1	-9.3	-7.4	-4.5	-2.6	-4.8	-5.8	-5.2	-4.7
9	Max	43.1	43.9	43.8	43.2	42.7	44.7	43.2	43.4	43.6	44.5	44.3	42.3
	Min	-7.1	-5.7	-1.7	-5.0	-5.0	-8.1	-3.2	-2.7	-2.3	-6.8	-3.9	-4.2

G.3.2 Surface Area of Core Samples Available for Evaporative Moisture Loss

Corroboration of the core surface area available for evaporation (297 cm²) used in the calculations in Section 6.2.2 is done by referencing drilling instructions that specify the diameter of core to be obtained and core logs that provide elevations of core top and bottom depths, from which the core lengths can be calculated. Core top and bottom depths were recorded in *Sample Management Facility, Core Processing Checklist* (YMP 1996 [DIRS 178714], 1995 [DIRS 178715]). Drilling instructions recorded in DTN: TM0000SD9SUPER.002 [DIRS 168542] (Subpart DRC.19960819.0022, requirement # 3.1.6) specifies minimum core diameter of 2.4 in (6.1 cm), and DTN: TMUSWSD1200095.001 [DIRS 178755] (subpart DRC.19960926.0092, requirement # 3.12.1) specifies core diameter of 2.4 in.

Core length information is recorded in the Core Processing Checklist of the Sample Management Facility. Specific information on cores retrieved from boreholes SD-12 and UZ-14 is recorded in *Sample Management Facility, Core Processing Checklist* (YMP 1996 [DIRS 178714], 1995 [DIRS 178715]) and listed in Table G-4. The geometric and arithmetic means of the core lengths are 11.9 and 14.1 cm, respectively. The corresponding core-surface areas are 287 and 329 cm², respectively. The unqualified surface of 297 cm² used in the calculations in Section 6.2.2 is within 50% of the corroborating surface areas calculated above and, therefore, meets the criteria for qualification of unqualified data provided in the data qualification plan (SNL 2006 [DIRS 178762]).

Table G-4. Lengths of Cores Retrieved from Wells SD-12 and UZ-14

Well	SMF ID	Top (ft)	Bottom (ft)	Length (cm)
SD-12 ^a	26480 ^a	13.4 ^a	13.7 ^a	9.144 ^a
SD-12 ^a	26481 ^a	13.7 ^a	14.2 ^a	15.24 ^a
UZ-14	28953	1,725.8	1,726.3	15.24
UZ-14	28954	1,726.3	1,726.6	9.144
UZ-14	28956	1,728.1	1,728.8	21.336
UZ-14	28957	1,728.5	1,728.8	9.144
UZ-14	28924	1,716.4	1,716.6	6.096
UZ-14	28925	1,716.6	1,717.1	15.24
UZ-14	28927	1,718.9	1,719.4	15.24
UZ-14	28928	1,719.4	1,719.6	6.096
UZ-14	28958	1,731	1,731.3	9.144

Table G-4. Lengths of Cores Retrieved from Wells SD-12 and UZ-14 (Continued)

Well	SMF ID	Top (ft)	Bottom (ft)	Length (cm)
UZ-14	28959	1,731.3	1,731.7	12.192
UZ-14	28945	1,721.9	1,722.4	15.24
UZ-14	28946	1,722.4	1,722.7	9.144
UZ-14	28948	1,723.3	1,723.6	9.144
UZ-14	28976	1,743	1,743.2	6.096
UZ-14	28977	1,743.2	1,743.7	15.24
UZ-14	28984	1,746.7	1,747.1	12.192
UZ-14	28985	1,747.1	1,747.8	21.336
UZ-14	28965	1,734.5	1,734.7	6.096
UZ-14	28966	1,734.7	1,735.1	12.192
UZ-14	28970	1,737.1	1,737.4	9.144
UZ-14	28971	1,737.4	1,737.9	15.24
UZ-14	28987	1,749.8	1,750.1	9.144
UZ-14	28988	1,750.1	1,750.6	15.24
UZ-14	28990	1,752.3	1,752.7	12.192
UZ-14	28991	1,752.7	1,753	9.144
UZ-14	28973	1,740.2	1,740.4	6.096
UZ-14	28974	1,740.4	1,740.8	12.192
UZ-14	29031	1,761.8	1,762.1	9.144
UZ-14	29032	1,762.1	1,762.7	18.288
UZ-14	29038	1,765.5	1,765.7	6.096
UZ-14	29039	1,765.7	1,766.1	12.192
UZ-14	29204	1,755.6	1,756	12.192
UZ-14	29205	1,756	1,757.8	54.864
UZ-14	29042	1,768	1,768.6	18.288
UZ-14	29043	1,768.6	1,770.8	67.056
UZ-14	29208	1,758.5	1,758.8	9.144
UZ-14	29209	1,758.8	1,759	6.096

Sources: ^aYMP 1996 [DIRS 178714]; all others, YMP 1995 [DIRS 178715].

G.3.3 Confidence for in situ Measurement of Water Potential

In situ water potentials were measured with thermocouple psychrometers. Corroborating data that support the 95% confidence for in situ measurement of water potential of 0.2 MPa is available in Thermocouple Psychrometer Calibration Control Forms. The calibration data for two psychrometers are recorded in DTN: GS950208312232.003 [DIRS 105572] (subparts MOL.19950412.0198 and MOL.19950412.0213). The sensors were calibrated in the ranges – 7.4098 to –0.0904 MPa and –6.7547 to –0.0904 MPa, respectively. There were 107 and 90 calibration points, respectively, for each of the sensors. Measurement errors were documented in the calibration records for each calibration point. The 95% confidence intervals range from 0.1031 to 0.1487 MPa and 0.1018 to 0.1043 MPa. The corroborating 95% confidence interval of in situ water potential measurements is within the interval used in the calculations in Section 6.2.2 (0.2 MPa) and, therefore, meets the criteria for qualification of unqualified data provided in the data qualification plan (SNL 2006 [DIRS 178762]).